



# HHS Public Access

Author manuscript

*Wiley Interdiscip Rev Nanomed Nanobiotechnol.* Author manuscript; available in PMC 2016 July 01.

Published in final edited form as:

*Wiley Interdiscip Rev Nanomed Nanobiotechnol.* 2015 July ; 7(4): 593–608. doi:10.1002/wnan.1326.

## Ultrasound Imaging Beyond the Vasculature with New Generation Contrast Agents

**Reshani H. Perera, PhD,**

Department of Radiology, Case Western Reserve University, Cleveland OH 44106, USA

**Christopher Hernandez,**

Department of Biomedical Engineering, Case Western Reserve University, Cleveland OH 44106, USA

**Haoyan Zhou, MS,**

Department of Biomedical Engineering, Case Western Reserve University, Cleveland OH 44106, USA

**Pavan Kota,**

Department of Biomedical Engineering, Case Western Reserve University, Cleveland OH 44106, USA

**Alan Burke, and**

Department of Biomedical Engineering, Case Western Reserve University, Cleveland OH 44106, USA

**Agata A. Exner, PhD**

Departments of Radiology and Biomedical Engineering, Case Western Reserve University, Cleveland OH 44106, USA, 216-844-3544

Agata A. Exner: [Agata.exner@case.edu](mailto:Agata.exner@case.edu)

### Abstract

Current commercially available ultrasound contrast agents are gas-filled, lipid- or protein-stabilized microbubbles larger than 1  $\mu\text{m}$  in diameter. Because the signal generated by these agents is highly dependent on their size, small yet highly echogenic particles have been historically difficult to produce. This has limited the molecular imaging applications of ultrasound to the blood pool. In the area of cancer imaging, microbubble applications have been constrained to imaging molecular signatures of tumor vasculature and drug delivery enabled by ultrasound-modulated bubble destruction. Recently, with the rise of sophisticated advancements in nanomedicine, ultrasound contrast agents, which are an order of magnitude smaller (100-500 nm) than their currently utilized counterparts, have been undergoing rapid development. These agents are poised to greatly expand the capabilities of ultrasound in the field of targeted cancer detection and therapy by taking advantage of the enhanced permeability and retention phenomenon of many tumors and can extravasate *beyond* the leaky tumor vasculature. Agent extravasation facilitates highly sensitive detection of cell surface or microenvironment biomarkers, which could advance early cancer detection. Likewise, when combined with appropriate therapeutic agents and

ultrasound-mediated deployment on demand, directly at the tumor site, these nanoparticles have been shown to contribute to improved therapeutic outcomes. Ultrasound's safety profile, broad accessibility and relatively low cost make it an ideal modality for the changing face of healthcare today. Aided by the multifaceted nano-sized contrast agents and targeted theranostic moieties described herein, ultrasound can considerably broaden its reach in future applications focused on the diagnosis and staging of cancer.

---

## Introduction

During the past two decades, the advent of microbubble ultrasound contrast agents (UCA) has enhanced the capabilities of ultrasound as a medical imaging modality and stimulated innovative strategies for cancer detection, therapy and post-therapy monitoring. While the utilization of microbubbles has shown encouraging results, their potential range of molecular imaging and targeted drug delivery applications in cancer diagnosis and therapy has been limited by a large hydrodynamic diameter (1-8  $\mu\text{m}$ ), which typically confines them to the vasculature. Bubbles produce contrast due to their variable response to changes in acoustic pressure. In essence, the bubbles “bounce” or vibrate - they shrink at high pressure and expand at low pressures. These vibrations can be linear or nonlinear (harmonic), and the acoustic impedance mismatch between host tissue and bubbles provides the contrast for ultrasound imaging. To augment their multifunctional capacity specific to cancer-related challenges, it is critical to reduce bubble size to the nanometer range without reducing visibility on ultrasound. This step would enable numerous new, paradigm shifting applications of these agents, particularly in cancer detection and therapy, since their activity could be explored in molecular imaging and site-specific drug delivery.

For many years, ultrasound imaging has been a consistently utilized tool in diagnosis and management of a broad range of diseases. However, while the cutting edge research in advancement of other imaging modalities (MRI, CT, PET and optical) in basic and translational areas of molecular imaging has flourished in the past decade, ultrasound has seen relatively slower progress. Ultrasound has numerous exciting advantages over other modalities, including wide availability, outstanding safety profile, lack of ionizing radiation, high spatial and temporal (real time) resolution, and portability. It is also low cost; according to a recent report, the cost factor for ultrasound is nearly 5 times lower than MRI and 3 times lower than CT. In the same study the authors conclude that up to \$736 million annually could be saved by replacing MRI with ultrasound for many standard studies<sup>1</sup>.

The ability to formulate robust sub-micron contrast agents able to penetrate deep into tissue, detect cell surface markers or molecules in the tissue, and to carry therapeutic agents for on-demand deployment is critical to development of ultrasound as a molecular imaging tool. Ultrasound detection with contrast agents has been described to have picomolar sensitivity – on par with optical and nuclear imaging<sup>2</sup>, yet the small size of highly echogenic (ultrasound-visible) agents has been elusive. Discoveries aimed at development of robust contrast agent formulations, and appropriate hardware and software that overcome these challenges will serve as a springboard for a new application of ultrasound. The primary focus of this review is recent innovation and development of contrast agents and therapeutic moieties which are

clearly visible with ultrasound yet sufficiently small to move beyond the leaky tumor vasculature, permitting greatly expanded molecular imaging capabilities of ultrasound in clinical and translational research applications.

## Physics and Theory behind Ultrasound and Its Contrast Agents

Ultrasound describes sound waves with frequencies (>20kHz) beyond the range of human hearing. Ultrasound as a medical imaging modality utilizes the propagation of the high frequency sound waves in organs and tissues of different acoustic properties to produce anatomic images. This is implemented by using a “pulse echo” technique where a short pulse of high frequency sound waves interacts with tissues mechanically to synthesize a grayscale image. A transducer generates the sound pulses and detects returning echoes, which also directs the ultrasound pulse along a linear path through the patient. Along this path, the depth of the imaging structure is determined by the time between firing the pulse and receiving the echo, and the amplitude of the echo is encoded and displayed in a grayscale image. In addition to two-dimensional tomographic imaging, ultrasound provides other functions such as blood velocity measurements using the concept of Doppler shift to measure the motion of blood. Both the velocity and direction of blood flow can be measured in this mode<sup>3</sup>.

The concept of contrast enhancement was introduced to ultrasound 40 years ago by an accidental discovery that an injection of indocyanine green to measure cardiac output consistently resulted in a transient signal increase. This was shown by subsequent research to be caused by formation of small air bubbles at the catheter tip during injection<sup>4</sup>. However, the effect of this “agent” was momentary and difficult to replicate, which limited its use in clinical practice. It was not until the 1980s that a new generation of stabilized gas bubbles was developed. Stabilizing methods included initially using albumin as the shell while filling the bubbles with air<sup>5</sup>. This resulted in the first pharmaceutical echo-enhancer, Alunex (Molecular Biosystems), which is no longer in use. Since then, various other shell materials such as proteins, lipids or polymers<sup>6</sup> have been investigated. Filling the bubbles with high molecular weight and low solubility gases like perfluorocarbons or sulphur hexafluoride instead of air can increase microbubble persistence in the circulation (Figure 1A).

Microbubbles act as echo-enhancers because of the high acoustic impedance mismatch between the blood and gas and due to their ability to resonate at frequencies within the clinical ultrasound range (2-10 MHz). The volumetric oscillation of bubbles when exposed to the compression-rarefaction sequence of an ultrasonic pulse provides a much stronger ultrasound signal than similar sized tissue reflectors such as red blood cells<sup>7, 8</sup>. Bubble compressibility also results in a more complex response to the ultrasound field compared to soft tissue. At low acoustic power (defined as the mechanical index, or  $MI < 0.1$ ), microbubbles oscillate symmetrically (Figure 1B). At intermediate acoustic power ( $0.1 < MI < 0.5$ ), microbubbles exhibit a nonlinear behavior where expansion and contraction phases become unequal because microbubbles resist compression more than expansion (Figure 1C). The return signal contains multiple echoes called harmonics. In comparison, tissue has a relatively linear behavior due to its incompressibility. This enables a unique

opportunity to tune signal processing and improve detection of the bubbles. At even higher acoustic power ( $MI > 0.5$ ), microbubbles can be destroyed, and the phenomenon can be beneficial to processes such as drug delivery (Figure 1D)<sup>4, 9, 10</sup>.

In order better detect microbubbles several ultrasound imaging sequences have been developed. For example, in contrast harmonic imaging, an ultrasound pulse is transmitted at the harmonic frequency but the return echo is received at twice this frequency, which results in larger bubble echo intensity than tissue and thus enhanced contrast. Unlike tissue, microbubbles experience nonlinear behavior when excited with ultrasound waves. Pulse/phase inversion imaging uses consecutive pulses with inverted phase to exploit this difference by summing their return echo<sup>11</sup>. Finally, a stimulated acoustic emission (SAE) sequence uses microbubble destruction high acoustic power to produce a strong but transient echo<sup>12</sup>.

In addition to the local acoustic field, physical bubble properties are key parameters affecting contrast efficiency. These factors are represented by the Equation (1)<sup>13-16</sup>, which arises from the small amplitude expansion of the Raleigh-Plesset equation. According to Equation (1), the resonant frequency of a microbubble is related to the bubble radius ( $R_0$ ) and the shell elasticity ( $\chi$ ).

$$f_0 = \frac{1}{2\pi R_0} \sqrt{\frac{1}{\rho_L} \left[ 3\gamma P_0 + \frac{2(3\gamma - 1)\sigma}{R_0} + \frac{4\chi}{R_0} \right]} \quad \text{Equation (1)}$$

Equation 1. Bubble resonance frequency.  $f_0$ : the resonant frequency of a microbubble,  $\gamma$ : the ratio of the specific heats of the gas inside the bubble,  $\rho_L$ : density of surrounding liquid,  $R_0$ : bubble radius,  $P_0$ : ambient fluid pressure,  $\sigma$ : the surface tension at the gas-liquid interface,  $\chi$ : the elasticity parameter of the shell.

Recently, smaller sub-micron ultrasound contrast agents have drawn intense research interest in not only diagnostic but also therapeutic applications, particularly in the area of oncology. Because these “nanobubbles” are small enough to extravasate through leaky tumor vasculature, they can more effectively reach cell targets to either highlight the lesion (diagnostic) or deliver their payload (therapeutic)<sup>17-21</sup>. However, as shown in Equation (1), the smaller the bubble size, the higher the resonant frequency and, subsequently, the higher the ultrasound frequency needed for detection. Similarly, increasing shell stiffness results in higher bubble resonant frequency. To circumvent this, high frequency (30 - 50MHz) small animal ultrasound systems have been used. For example, Lanza et al. used a 30MHz intravascular ultrasound system to detect thrombi with a targeted perfluorocarbon emulsion based contrast agent (250nm)<sup>22</sup>. Wang et al. used a custom-made 40MHz transducer to image nanobubbles (485nm) targeting to CCRF-CEM cells in an *ex vivo* model<sup>23</sup>. Efforts have also been made to decrease the shell stiffness by incorporating surfactant in order to decrease the detection frequency for nanobubbles, as described in detail below<sup>18</sup>.

## Clinical Applications of Ultrasound Contrast Agents

Ultrasound contrast agents have applications primarily in noninvasive cardiovascular imaging, including echocardiography, and quantifying tissue perfusion and microvascular blood flow and blood volume<sup>24</sup>. UCAs have also been applied in imaging of the carotid artery lumen (contrast-enhanced carotid ultrasound) and of atherosclerotic plaque neovascularization<sup>24, 25</sup>, which also serve as possible foci of future drug-delivery systems. Currently, two microbubble products are approved by the Food and Drug Administration (FDA) for use in the United States: Optison (GE Healthcare, Buckinghamshire, UK), since 1997, and Definity<sup>®</sup> (Lantheus Medical Imaging, North Billerica, MA), since 2001. They are indicated for and commonly used to improve the quality of echocardiograms, by opacification of left heart structures. Other agents used in Europe, such as Echovist<sup>24</sup>, improve quality of signals in the venous vascular bed and right heart (Table 1). The main application of contrast-enhanced ultrasound (CEUS) in Europe is detection and characterization of focal liver lesions. CEUS is also used this way in Japan, but the FDA has not approved CEUS for liver application in the United States<sup>26</sup>.

While evidence increasingly suggests that UCAs may not significantly contribute to adverse effects including cardiopulmonary complications, there have been reports to the FDA of serious issues post-administration, including several deaths related to commonly-used UCAs. In 2007, Definity<sup>®</sup> and Optison were assigned FDA black box warnings suggesting risk for severe cardiopulmonary reactions. These have since been partially relaxed, but still recommend a 30 minute minimum monitoring period for patients with pulmonary hypertension or unstable cardiopulmonary condition. However, more-recent surveillance and analysis indicate that Definity<sup>®27, 28</sup> and Optison<sup>28</sup> may not increase the risk for adverse cardiopulmonary reactions across several demographics, including age, BMI, and severity of cardiopulmonary condition. It is also suggested<sup>28</sup> that severe adverse effects are no more likely to occur in imaging tests utilizing these agents than in other cardiac imaging tests.

SonoVue (Bracco, Milan, Italy), a second generation UCA, has applications in Doppler and echocardiography<sup>29</sup>, and possibly diagnosis of vesicoureteral reflux<sup>30</sup>. While it has not been approved by the FDA, it shows a safety profile comparable to approved UCAs, with adverse effects seen in 0.47% of patients, where 0.08% were drug-related. SonoVue appears to have no significant effect on pulmonary hemodynamics, cardiac or pulmonary function, blood pressure, oxygen saturation, or electrocardiographic parameters. Although the FDA has acknowledged that risks associated with UCAs were less severe than previously believed, the black box warning for commercially available UCAs remains, but has been considerably relaxed, and several contraindications have been removed.

While UCAs for diagnosis of heart related issues have been well established in the clinic, other applications have also shown potential in clinical studies in recent years. Microbubbles for diagnosis and treatment of breast, prostate, and liver cancer, among others, have been tested in clinical trials with promising results<sup>24</sup>. Sonazoid<sup>®</sup> microbubbles were shown to improve the accuracy of diagnosis of prostate cancer, which could reduce the number of biopsies patients need to receive to achieve a similar diagnostic result<sup>31</sup>. In Japan, Sonazoid<sup>®</sup> was also used in a phase III clinical trial to compare its diagnostic potential of

focal breast lesions against unenhanced ultrasound and contrast enhanced MRI (Figure 2)<sup>32</sup>. The study found that while CEUS technology did not statistically significantly increase the sensitivity of the diagnosis, it substantially enhanced the accuracy and specificity at a reduced cost<sup>32</sup>. UCAs can also be used in conjunction with commercially available clinical ultrasound scanners to induce sonoporation. Sonoporation is an experimental technique that facilitates the cellular uptake of drugs by using sound waves to form pores in cell membranes. A recent clinical case study utilized SonoVue<sup>®</sup> microbubbles with the chemotherapy treatment gemcitabine and demonstrated an ability to reduce tumors to 70 ± 5% of their original size in patients with pancreatic adenocarcinoma<sup>33</sup>.

## Next Generation Nano Agents in Cancer Detection

Although microbubbles have had recent clinical success in cancer diagnostics, their relatively large hydrodynamic radius (1-8 μm) has limited their applications to the vasculature and thus has sparked interest in reducing the size of the echogenic bubbles to the nanoscale. The recent interest surrounding sub-micron UCAs can be attributed to their ability to exploit the enhanced permeability and retention (EPR) effect, which is the leaky vasculature and imperfect lymphatic drainage associated with cancerous tissue. The imperfect vasculature varies by tumor type, but typically allows for particles smaller than 400 nm to accumulate within a tumor, although a maximized transition effect has been found with particles less than 200 nm<sup>19</sup>. Despite the benefits associated with nano-UCAs, translation into the clinical setting has been hindered by challenges with the nanoparticle formulations such as echogenicity at clinically relevant ultrasound frequencies (1-10 MHz), and time and cost effective scale up formulations. Despite these limitations, prolific research in the area has resulted in various nanoparticle formulations that have circumvented these issues and enabled their application as diagnostic and therapeutic agents.

Reducing the size of a microbubble into a nanobubble reduces not only its echogenicity under clinical ultrasound, but also the stability of the bubble in solution. Bubble stability is related to the counteractive forces of the partial pressures of dissolved gasses in the surrounding fluid and the sum of the Laplace pressure and ambient pressure<sup>34</sup>. According to Equation (2), the Laplace (  $P$  ) increases with decreasing radius (R), reducing the stability of the bubble.

$$\Delta P = (P_b - P_a) = \frac{2\sigma}{R} \quad \text{Equation (2)}$$

Equation 2.  $P$ : Laplace pressure,  $P_b$ : total pressure inside bubble,  $P_a$ : ambient pressure outside of bubble,  $\sigma$ : surface tension at gas-bubble interface, R: bubble radius.

The addition of surfactants or lipids helps to stabilize nanobubbles by acting as an elastic shell to counteract the effect of surface tension. Selection of the gas core in a nanobubble is also critical to its stability. The use of a perfluorocarbon gas core rather than air, nitrogen or sulfurhexafluoride — all commonly used gasses in microbubble formulations — decreases bubble dissolution time due its low solubility in blood.

The ideal nano-UCA should have an appropriate circulation half-life, on the order of hours for imaging applications to several days for therapeutic applications, to allow for accumulation of the particles at the targeted site<sup>35</sup>. In order to increase circulation time, formulations should be stable in solution (i.e. resist aggregation) and avoid reticuloendothelial (RES) uptake. The overall surface charge that a particle acquires in a medium, indirectly measured as the zeta potential, can provide a repulsive force between particles, thereby reducing the propensity for aggregation or flocculation. When designing nanoparticle formulations it is important for particles to have a high zeta potential ( $\pm 30\text{mV}$ ) for particles stabilized solely on repulsion<sup>36</sup>. Incorporation of polyethylene glycol (PEG) as a steric hinderer on the surface of nanoparticles has also been shown to increase circulation time by reducing opsonization and clearance by the RES<sup>37</sup>. In a study looking at the effect of pegylation on poly(lactic-co-glycolic acid (PLGA) nano-UCA's, pegylation of nanoparticles led to an *in vitro* reduction of the complement activation system and an increase in particle accumulation within a tumor *in vivo*<sup>38</sup>.

Several techniques to reduce the size of microbubbles and meet criteria described above have been investigated. The most frequently investigated is post-formulation separation. Traditional single layer lipid or surfactant encapsulated bubbles are polydisperse with a mean size around 1-2  $\mu\text{m}$  in diameter regardless of agitation protocol<sup>39</sup>. Although the mechanism is not fully understood, it has been postulated that the shell bending modulus resists increases in curvature below 1  $\mu\text{m}$ , producing only a small number of nanobubbles<sup>39</sup>. Nanobubble formulations have thus been obtained by extraction of this nanometer subpopulation from microbubble solutions based on their buoyancy by centrifugation<sup>23, 40-45</sup>. Although this method produces a relatively small nanobubble yield, it has been demonstrated that these nanobubbles are capable of extravasating the leaky vasculature in tumors and improving signal intensity under diagnostic ultrasound<sup>42-44</sup>. In a recent study, Fan et al. (2013) compared the echogenicity and signal intensity of commercially available SonoVue<sup>®</sup> microbubbles against their lipid based nanobubbles (mean diameter  $435.2 \pm 63.53\text{nm}$ ) accumulating at a gastric cancer site in a mouse model<sup>44</sup>. When compared *in vivo*, inside the gastric cancer xenografts, the nanoparticles had significantly higher peak signal intensity but had a slower arrival time and peak time than the microbubbles. The lag time in arrival time and time to peak was attributed to the nanobubbles slowly penetrating the tumor via their leaky vasculature that also resulted in the higher peak intensity.

Although post formulation manipulations of particle solutions, such as the centrifugation fractionation methods describe earlier, are effective in formation of nano-sized particle distributions, these methods are labor-intensive, wasteful of raw materials, and capable of only producing low particle yields. In order to produce echogenic nanoparticles directly, several groups have experimented with different particles formulations including lipid bilayer particles<sup>46-48</sup>, also known as liposomes, polymeric-shelled particles<sup>38, 49, 50</sup>, and Pluronic incorporated lipid shells<sup>17-19</sup>. These direct nanoparticle formulations are more practical for clinical translation as most of their sample preparation can be done prior to the clinical setting.

Our group has recently developed a direct nanobubble formulation through the use of a surfactant as a size modulator to produce bubbles as small as 100 nm<sup>17-19</sup>. The innovation of these agents lies in the surfactant-stabilized lipid shell. We hypothesize that the nonionic surfactant, Pluronic, changes the packing of the lipids in the shell and reduces the size of the bubbles to 100 nm or below (Figure 3A) but yet retains their echogenicity at a level comparable to clinical agents<sup>17</sup>. Pluronics, (also known as poloxamers), or polyethylene oxide (EO<sub>x</sub>)-polypropylene oxide (PO<sub>y</sub>)-polyethylene oxide (EO<sub>x</sub>), (where the x and y values differ to each type of Pluronic), are a family of nonionic triblock copolymers that are typically classified as inactive excipients by the FDA. These amphiphilic surfactants are commonly used in pharmaceutical and cosmetic applications as antifoaming agents and emulsifiers. Due to their widespread use, they are low cost, well studied and could result in more rapid translation of the developed contrast agent to clinical use. The extravasation capabilities and ultrasound contrast of these Pluronic-stabilized nanobubbles have been compared to that of lipid microbubbles without Pluronic in a 4T1 breast cancer model in mice (Figure 3B, C – unpublished data). Histological analysis suggests that the small nanobubbles or their fragments can extravasate out of the vasculature into the tumor tissue.

Echogenic liposomes, or ELIPs, unlike the monolayer bubbles described earlier, are lipid bilayer nanoparticles that contain small amounts of inert gas in their lipid bilayer or in micelles within their aqueous core. The ELIP is produced by introducing gas pockets inside the liposomes that formed by dehydration and rehydration technique. Briefly, the method includes hydration of lipid film, freezing the hydrated liposome solution in the presence of mannitol, lyophilization, and rehydration<sup>51, 52</sup>. When surface-modified with PEG, liposomes have great stability, biocompatibility, and long circulation time and can be easily prepared with great control over size and surface-modifications. Due to their gas core, as well as other advantages, these particles have been proposed as potential contrast agents for clinical ultrasound<sup>46-48</sup>. Despite their attractive benefits, echogenic liposomes for purely diagnostic purposes have not experienced great success in clinical translation. Their small size, low gas density and rigid shell do not allow for high contrast under ultrasound at diagnostic frequencies.

Polymeric shelled nanobubbles have been proposed as an alternative to lipid nanobubbles<sup>38, 49, 50</sup>. These nanoparticles are often made from biodegradable PLGA, or poly-L-lactide (PLLA) polymers, both of which have demonstrated biocompatibility and have been used in many FDA-approved devices. In one study by Rapoport et al, polymeric PEG-PLLA nanodroplets were generated with perfluoropentane at their center<sup>50</sup>. These particles remain as droplets at room temperature— due to perfluoropentane's boiling point under Laplacian pressure— and transition into gas particles at *in vivo* temperatures. These nanodroplets were able to produce strong ultrasound signal 4 hours after intravenous injection in the middle of a tumor with no signal in the kidneys or liver, suggesting high tumor selectivity. Biocompatible polymers can also serve as crosslinking agents to help stabilize the shell of nano contrast agents. In a recent studies, a chitosan cross-linked vitamin C lipid nanobubble was explored as a dual imaging (ultrasound-fluorescence) contrast agent<sup>53</sup>. The negative charge of the chitosan-vitamin C shell was shown to reduce the non-specific distribution of particles and improve tumor accumulation under ultrasound and



fluorescence imaging. Figure 4 shows the enhanced ultrasound contrast after injection of chitosan nanobubbles.

Molecular imaging, which enables the visualization of cellular functions or markers, has shown promise in improvement of contrast-enhanced diagnosis. Conjugation of targeting moieties, such as antibodies or peptides, to microbubbles has been shown to have potential applications in molecular diagnosis of vascular diseases such as atherosclerosis<sup>54</sup>. Since the advent of echogenic nanoparticles, molecular detection of cancer in animal models with ultrasound imaging has been demonstrated<sup>23, 47, 55</sup>. Nanoparticles can first reach tumor sites via their size-dependent passive targeting, and then, with the appropriate targeting ligand, can be coupled onto cancerous cells via overexpressed markers. These markers include HER2 and EGFR<sup>56</sup>. Common linking chemistries for the attachment of antibodies include biotin-avidin attachment, NHS/EDC- amine attachment, and maleimide-thiol attachment. Although useful for preclinical targeting studies, the potential immunogenic effects from biotin-avidin attachment prohibit its translation into humans. In a recent study, a cancer specific aptamer was conjugated to the lipid shell of nanobubbles and evaluated for its targeted imaging potential<sup>23</sup>. Using a high frequency transducer (40 MHz) and c-mode imaging, a monolayer of cancer cells with bound targeted nanobubbles could be visualized using ultrasound imaging.

### Therapeutic Applications of Nano-scale Ultrasound Contrast Agents

Complementary to diagnostic imaging, recent advances in nanomedicine have attracted significant attention in the development of co-functionalized agents that can achieve both diagnostic and therapeutic functionality. These nano-theranostics have additional advantages including the ability to monitor the tumor accumulation and biodistribution of the active agent, capacity to actively trigger drug release with both spatial and temporal specificity, and a means to concurrently assess therapeutic efficacy via perfusion and molecular imaging. Among all on-demand image guided drug delivery techniques, ultrasound has become the frontrunner due to its wide availability, capacity for real-time analysis, non-invasive application, low cost, and ease of usage with local applicability with highly proven safety.

The traditional ultrasound drug delivery strategies are based on combining unloaded UCA (mostly microbubbles) with the nanoscale therapeutic agents. The small therapeutic agent can penetrate into the intracellular space due to cavitation and increased permeability of cellular membrane with the assistance of ultrasound<sup>57-60</sup>. In this regard, development of nanosized, drug loaded UCA in a single system is beneficial for both imaging and localized drug delivery due to transient increase in permeability of vasculature and cellular membrane. Nano-scale echogenic carrier systems for therapeutic strategies can be categorized as liposomes, polymers, micelles, and a hybrid of one or two of the above.

Liposomes, as lipid based nanocarriers, have gained a growing amount of advantages due to their controllable size, ability to modify the surface with targeting moieties, and encapsulation efficiency of therapeutic agents. Liposomes can be loaded with both hydrophilic and hydrophobic drugs by formation in aqueous solution saturated with soluble

drug, solvent exchange mechanism, and pH gradient methods<sup>61</sup>. Several studies showed that drug release from liposomes could be triggered by various techniques including ultrasound at clinically relevant frequencies<sup>62-67</sup>. Consequently, development of an agent combining liposome and contrast, or echogenic liposome (ELIP), is an ideal candidate in ultrasound molecular imaging and ultrasound triggered drug delivery. Such acoustically active liposomes have been used for ultrasound based theranostic applications by encapsulating agents such as drugs, antigens, and genes<sup>68-71</sup>. However, most reported studies show success with hydrophilic drugs, while hydrophobic drugs tend to remain in the reorganized lipid layer upon ultrasound release<sup>71</sup>.

Nano-sized, polymer-based, perfluorocarbon UCAs have been extensively investigated for enhanced nanomedicine applications in cancer diagnosis and therapy. In these approaches, the polymeric nanoparticle core is loaded with a variety of therapeutic agents in addition to the imaging agent. As mentioned earlier, the Rapoport group developed a drug loaded poly(ethylene oxide)-co-poly(D,L-lactide) nanoemulsions that can convert into microbubbles by the action of ultrasound, which ultimately releases the encapsulated drugs<sup>72-76</sup>. On the other hand, polymeric micro-sized UCAs were developed with poly(lactic acid)(PLA), which demonstrated dramatic size reduction (~350nm) and payload release as a response to external focus ultrasound<sup>77</sup>. These resulting nano-sized particles can easily pass through the leaky vasculature within the tumor. In related studies, drug-loaded nanoscale PLGA polymer-stabilized bubbles were synthesized using a double emulsion evaporation method and used for on-demand drug release with high intensity focused ultrasound (HIFU)<sup>78</sup>. Such polymeric nanocarriers have demonstrated enhanced therapeutic efficacy with improved therapeutic index of systemically administered chemotherapeutic agents, such as doxorubicin (Dox), methotrexate, and paclitaxel, with reduced drug accumulation in healthy organs<sup>50, 77-82</sup>.

As an alternative to the bilayer, lipid based nanobubbles, our group has developed monolayered, lipid shelled nanobubbles stabilized with the surfactant Pluronic, as described above<sup>19</sup>. The size of the bubbles was reduced due to the incorporation of the Pluronic into the shell<sup>17, 18</sup>. Our prior work has shown that Pluronic, in addition to having attractive structural properties can also be a highly bioactive molecule and can impart a thermosensitizing effect in tumors to reduce the temperature required to achieve cell death via techniques such as thermal ablation or low grade hyperthermia<sup>83, 84</sup>. Accordingly, Pluronic incorporated into the nanobubble shell serves both as a structural stabilizer and the active agent when combined with hyperthermia. The Pluronic nanobubble has demonstrated enhanced contrast and site-specific ultrasound-mediated Pluronic release for enhanced thermal ablation *in vivo*<sup>83, 84</sup>. Figure 5 shows the theranostic strategy of Pluronic nanobubbles for enhanced hyperthermia. In our current studies, we are further improving the formulation by adding an interpenetrating crosslinking agent into the hydrophobic core of nanobubbles (Figure 6A). The stabilizing agent, N-N-Diethyacylamide, forms a network that can entangle the hydrophobic part of lipids and Pluronic without any chemical reaction<sup>66</sup>. Furthermore, the stabilizing agent is biodegradable and proven to increase the circulation time in polymeric micelles. The new design of Pluronic bubbles shows the

enhanced echogenicity and the low ultrasound decay rate compared to the uncross-linked Pluronic bubbles (Figure 6B, C –unpublished data).

The most recent development of lipid-based theranostic agents has been the formulation of emulsion liposomes (eLiposomes) that can encapsulate drugs or genes. These eLiposomes are composed of perfluoropentane nanodroplets within the aqueous core of phospholipid liposomes. Such eLiposomes are sensitive for low intensity ultrasound at 20 kHz and have the capability to release the payload upon ultrasound application<sup>85, 86</sup>. Polymeric micelles combined with lipid shelled bubbles have also been developed as ultrasound-sensitive theranostic nanocarriers for siRNA for tumor gene therapy<sup>87</sup>. In another approach, gold nanoparticles and gold shell nanocapsules were utilized as theranostic agents for image-guided photothermal therapy for cancer<sup>88-91</sup>. In this case, the perfluorooctylbromide (PFOB) was incorporated as the contrast agent, which enhanced ultrasound echogenicity for diagnostic purposes and located the disease site for enhanced tumor ablation. In related studies, mesoporous silica nanoparticles (MSNs) functionalized with the tumor specific targeting and loading therapeutic agent have also been developed for ultrasound imaging and therapy for various cancer models<sup>50, 92-95</sup>. These stable and biocompatible MSNs are localized and bind to the targeted site and release the payload drugs. Furthermore, the UCAs were able to couple to paramagnetic compounds, such as superparamagnetic iron oxide nanoparticle (SPIOs), to produce bi-functional agents that have both ultrasound and MRI imaging capability for tumor treatments<sup>88, 89, 96, 97</sup>. The bimodal imaging platform provides excellent diagnosis information and precise location for the therapeutic focusing spot for photothermal therapy.

## Conclusion

Ultrasound is the least expensive, yet arguably the most robust clinical imaging modality. The low price point, high safety profile and wide availability make ultrasound ideal for delivering targeted imaging agents and image-guided therapeutics to populations that would not otherwise have access to such technology. The potential impact of this field on the course of healthcare reform is of enormously high significance. Sub-micron UCAs, such as the ones summarized here, have been the subject of much recent research. If successfully advanced beyond the laboratory, these agents will fulfil an urgent, unmet need for new cancer-specific UCAs and therapeutics. Since ultrasound is already utilized in cancer screening, and often the contrast agents are comprised of molecules already approved for use in humans in other applications, the timeline for translation of this technology from lab to life could be considerably shortened from the typical expected duration of a new pharmaceutical entity.

Some challenges remain. The foremost is development of appropriate software and hardware that will be utilized especially for the detection of small targeted nanoparticles at the target site. Although behavior of microbubbles within the blood pool is well understood, their performance will undoubtedly be altered within tissue. How UCAs will be best detected in this constrained environment and when bound to or internalized by cells where their resonant frequency will almost with certainty be affected, remains to be determined. Another related issue is development of the detection techniques and software algorithms

that can best identify those agents that are specifically bound to their target versus simply located within a tissue volume. The ability to do both in three dimensions and in real time would provide unprecedented opportunities for use of UCAs in cancer detection and quantification of processes such as tumor perfusion. Finally, hardware and software for ultrasound-mediated release of therapeutics at the target site, although currently available, will need to undergo refinement specific to nano-UCAs. Here, development of transducers capable of both imaging and deployment concurrently and in three dimensions would be most desirable. On the formulation front, continued development of targeted small, yet highly echogenic formulations with a prolonged stability and thus longer circulation time, is of paramount importance. For drug delivery applications, development of carriers with increased cargo capacity to maximize drug loading will yield more efficient, therapeutically relevant strategies in cancer therapy. Continued fruitful research into these areas will pave the path for exciting future applications of molecular imaging and personalized medicine with ultrasound and stands to make this promising technology available to a much greater population than the current expensive and complex molecular imaging strategies.

## Acknowledgments

This work was supported by the National Cancer Institute of the National Institutes of Health under award number R01CA136857 and by the Department of Defense Ovarian Cancer Research Program under award number DOD-WX81XWH-12-1-0500. Views and opinions of, and endorsements by the author(s) do not reflect those of the US Army or the Department of Defense or the National Institutes of Health.

## References

1. Parker L, Nazarian L, Carrino J, Morrison W, Grimaldi G, Frangos A, Levin D, Rao V. Musculoskeletal imaging: medicare use, costs, and potential for cost substitution. *J Am Coll Radiol*. 2008; 5:182–188. [PubMed: 18312965]
2. Roach M 3rd, Alberini JL, Pecking AP, Testori A, Verrecchia F, Soteldo J, Ganswindt U, Joyal JL, Babich JW, Witte RS, et al. Diagnostic and therapeutic imaging for cancer: therapeutic considerations and future directions. *J Surg Oncol*. 2011; 103:587–601. [PubMed: 21480253]
3. Bushberg, JT.; Seibert, A.; Leidholdt, E.; Boone, J. *The Essential Physics of Medical Imaging*. Philadelphia: Lippincott Williams & Wilkins; 2002.
4. Calliada F, Campani R, Bottinelli O, Bozzini A, Sommaruga MG. Ultrasound contrast agents: basic principles. *Eur J Radiol*. 1998; 27(Suppl 2):S157–160. [PubMed: 9652516]
5. Feinstein SB, Ten Cate FJ, Zwehl W, Ong K, Maurer G, Tei C, Shah PM, Meerbaum S, Corday E. Two-dimensional contrast echocardiography. I. In vitro development and quantitative analysis of echo contrast agents. *J Am Coll Cardiol*. 1984; 3:14–20. [PubMed: 6690542]
6. Quaia E. Microbubble ultrasound contrast agents: an update. *Eur Radiol*. 2007; 17:1995–2008. [PubMed: 17351779]
7. Phillips P, Gardner E. Contrast-agent detection and quantification. *Eur Radiol*. 2004; 14(Suppl 8):P4–10. [PubMed: 15700327]
8. Stride E, Saffari N. Microbubble ultrasound contrast agents: a review. *Proc Inst Mech Eng H*. 2003; 217:429–447. [PubMed: 14702981]
9. Cosgrove D. Ultrasound contrast agents: an overview. *Eur J Radiol*. 2006; 60:324–330. [PubMed: 16938418]
10. Correas JM, Bridal L, Lesavre A, Mejean A, Claudon M, Helenon O. Ultrasound contrast agents: properties, principles of action, tolerance, and artifacts. *Eur Radiol*. 2001; 11:1316–1328. [PubMed: 11519538]

11. Simpson DH, Chin CT, Burns PN. Pulse inversion Doppler: A new method for detecting nonlinear echoes from microbubble contrast agents. *Ieee Transactions on Ultrasonics Ferroelectrics and Frequency Control*. 1999; 46:372–382.
12. Blomley MJK, Albrecht T, Cosgrove DO, Eckersley RJ, Butler-Barnes J, Jayaram V, Patel N, Heckemann RA, Bauer A, Schlieff R. Stimulated acoustic emission to image a late liver and spleen-specific phase of Levovist(R) in normal volunteers and patients with and without liver disease. *Ultrasound in Medicine and Biology*. 1999; 25:1341–1352. [PubMed: 10626621]
13. de Jong N, Hoff L, Skotland T, Bom N. Absorption and scatter of encapsulated gas filled microspheres: theoretical considerations and some measurements. *Ultrasonics*. 1992; 30:95–103. [PubMed: 1557838]
14. Jong ND, Cornet R, Lancee CT. Higher harmonics of vibrating gas-filled microspheres. Part one: simulations *Ultrasonics*. 1994; 32:447–453.
15. Yanjun G, Cabodi M, Porter T. Pressure-dependent resonance frequency for lipid-coated microbubbles at low acoustic pressures. *Ultrasonics Symposium (IUS), 2010 IEEE*. 2010
16. Doinikov AA, Haac JF, Dayton PA. Resonance frequencies of lipid-shelled microbubbles in the regime of nonlinear oscillations. *Ultrasonics*. 2009; 49:263–268. [PubMed: 18977009]
17. Wu H, Rognin NG, Krupka TM, Solorio L, Yoshiara H, Guenette G, Sanders C, Kamiyama N, Exner AA. Acoustic characterization and pharmacokinetic analyses of new nanobubble ultrasound contrast agents. *Ultrasound Med Biol*. 2013; 39:2137–2146. [PubMed: 23932272]
18. Krupka TM, Solorio L, Wilson RE, Wu H, Azar N, Exner AA. Formulation and characterization of echogenic lipid-Pluronic nanobubbles. *Mol Pharm*. 2010; 7:49–59. [PubMed: 19957968]
19. Perera RH, Solorio L, Wu H, Gangolli M, Silverman E, Hernandez C, Peiris PM, Broome AM, Exner AA. Nanobubble ultrasound contrast agents for enhanced delivery of thermal sensitizer to tumors undergoing radiofrequency ablation. *Pharm Res*. 2014; 31:1407–1417. [PubMed: 23943542]
20. Wang Y, Li X, Zhou Y, Huang P, Xu Y. Preparation of nanobubbles for ultrasound imaging and intracellular drug delivery. *Int J Pharm*. 2010; 384:148–153. [PubMed: 19781609]
21. Suzuki R, Takizawa T, Negishi Y, Utoguchi N, Maruyama K. Effective gene delivery with novel liposomal bubbles and ultrasonic destruction technology. *Int J Pharm*. 2008; 354:49–55. [PubMed: 18082343]
22. Lanza GM, Wallace KD, Fischer SE, Christy DH, Scott MJ, Trousil RL, Cacheris WP, Miller JG, Gaffney PJ, Wickline SA. High-frequency ultrasonic detection of thrombi with a targeted contrast system. *Ultrasound Med Biol*. 1997; 23:863–870. [PubMed: 9300990]
23. Wang CH, Huang YF, Yeh CK. Aptamer-conjugated nanobubbles for targeted ultrasound molecular imaging. *Langmuir*. 2011; 27:6971–6976. [PubMed: 21553884]
24. Feinstein SB. The powerful microbubble: from bench to bedside, from intravascular indicator to therapeutic delivery system, and beyond. *Am J Physiol Heart Circ Physiol*. 2004; 287:H450–457. [PubMed: 15277188]
25. Shah F, Balan P, Weinberg M, Reddy V, Neems R, Feinstein M, Dainauskas J, Meyer P, Goldin M, Feinstein SB. Contrast-enhanced ultrasound imaging of atherosclerotic carotid plaque neovascularization: a new surrogate marker of atherosclerosis? *Vasc Med*. 2007; 12:291–297. [PubMed: 18048465]
26. Claudon M, Dietrich CF, Choi BI, Cosgrove DO, Kudo M, Nolsoe CP, Piscaglia F, Wilson SR, Barr RG, Chammas MC, et al. Guidelines and Good Clinical Practice Recommendations for Contrast Enhanced Ultrasound (Ceus) in the Liver - Update 2012 a Wfumb-Efsumb Initiative in Cooperation with Representatives of Afsumb, Aium, Asum, Flaus and Icus. *Ultrasound in Medicine and Biology*. 2013; 39:187–210. [PubMed: 23137926]
27. Weiss RJ, Ahmad M, Villanueva F, Schmitz S, Bhat G, Hibberd MG, Main ML. CaRES (Contrast Echocardiography Registry for Safety Surveillance): a prospective multicenter study to evaluate the safety of the ultrasound contrast agent definity in clinical practice. *J Am Soc Echocardiogr*. 2012; 25:790–795. [PubMed: 22560734]
28. Wei K, Mulvagh SL, Carson L, Davidoff R, Gabriel R, Grimm RA, Wilson S, Fane L, Herzog CA, Zoghbi WA, et al. The safety of Definity and Optison for ultrasound image enhancement: a

- retrospective analysis of 78,383 administered contrast doses. *J Am Soc Echocardiogr.* 2008; 21:1202–1206. [PubMed: 18848430]
29. Galema TW, Geleijnse ML, Vletter WB, de Laat L, Michels M, Ten Cate FJ. Clinical usefulness of SonoVue contrast echocardiography: the Thoraxcentre experience. *Neth Heart J.* 2007; 15:55–60. [PubMed: 17612661]
30. Papadopoulou F, Ntoulia A, Siomou E, Darge K. Contrast-enhanced voiding urosonography with intravesical administration of a second-generation ultrasound contrast agent for diagnosis of vesicoureteral reflux: prospective evaluation of contrast safety in 1,010 children. *Pediatr Radiol.* 2014; 44:719–728. [PubMed: 24442338]
31. Uemura H, Sano F, Nomiya A, Yamamoto T, Nakamura M, Miyoshi Y, Miki K, Noguchi K, Egawa S, Homma Y, et al. Usefulness of perflubutane microbubble-enhanced ultrasound in imaging and detection of prostate cancer: phase II multicenter clinical trial. *World J Urol.* 2013; 31:1123–1128. [PubMed: 22311543]
32. Miyamoto Y, Ito T, Takada E, Omoto K, Hirai T, Moriyasu F. Efficacy of Sonazoid (Perflubutane) for Contrast-Enhanced Ultrasound in the Differentiation of Focal Breast Lesions: Phase 3 Multicenter Clinical Trial. *American Journal of Roentgenology.* 2014; 202:W400–W407. [PubMed: 24660739]
33. Kotopoulos S, Dimcevski G, Gilja OH, Hoem D, Postema M. Treatment of human pancreatic cancer using combined ultrasound, microbubbles, and gemcitabine: A clinical case study. *Medical Physics.* 2013; 40
34. Quaia, E. *Contrast Media in Ultrasonography Basic Principles and Clinical Applications.* New York: Springer; 2005.
35. Jokerst JV, Lobovkina T, Zare RN, Gambhir SS. Nanoparticle PEGylation for imaging and therapy. *Nanomedicine (Lond).* 2011; 6:715–728. [PubMed: 21718180]
36. Muller RH, Jacobs C, Kayser O. Nanosuspensions as particulate drug formulations in therapy Rationale for development and what we can expect for the future. *Advanced Drug Delivery Reviews.* 2001; 47:3–19. [PubMed: 11251242]
37. Photos PJ, Bacakova L, Discher B, Bates FS, Discher DE. Polymer vesicles in vivo: correlations with PEG molecular weight. *J Control Release.* 2003; 90:323–334. [PubMed: 12880699]
38. Diaz-Lopez R, Tsapis N, Santin M, Bridal SL, Nicolas V, Jaillard D, Libong D, Chaminade P, Marsaud V, Vauthier C, et al. The performance of PEGylated nanocapsules of perfluorooctyl bromide as an ultrasound contrast agent. *Biomaterials.* 2010; 31:1723–1731. [PubMed: 19948357]
39. Kwan JJ, Borden MA. Lipid monolayer collapse and microbubble stability. *Adv Colloid Interface Sci.* 2012; 183-184:82–99. [PubMed: 22959721]
40. Xing Z, Wang J, Ke H, Zhao B, Yue X, Dai Z, Liu J. The fabrication of novel nanobubble ultrasound contrast agent for potential tumor imaging. *Nanotechnology.* 2010; 21:145607. [PubMed: 20220227]
41. Wheatley MA, Forsberg F, Dube N, Patel M, Oeffinger BE. Surfactant-stabilized contrast agent on the nanoscale for diagnostic ultrasound imaging. *Ultrasound Med Biol.* 2006; 32:83–93. [PubMed: 16364800]
42. Tong HP, Wang LF, Guo YL, Li L, Fan XZ, Ding J, Huang HY. Preparation of protamine cationic nanobubbles and experimental study of their physical properties and in vivo contrast enhancement. *Ultrasound Med Biol.* 2013; 39:2147–2157. [PubMed: 23932278]
43. Yin T, Wang P, Zheng R, Zheng B, Cheng D, Zhang X, Shuai X. Nanobubbles for enhanced ultrasound imaging of tumors. *Int J Nanomedicine.* 2012; 7:895–904. [PubMed: 22393289]
44. Fan XZ, Wang LF, Guo YL, Tong HP, Li L, Ding J, Huang HY. Experimental investigation of the penetration of ultrasound nanobubbles in a gastric cancer xenograft. *Nanotechnology.* 2013; 24
45. Oeffinger BE, Wheatley MA. Development and characterization of a nano-scale contrast agent. *Ultrasonics.* 2004; 42:343–347. [PubMed: 15047309]
46. Huang SL, Hamilton AJ, Pozharski E, Nagaraj A, Klegerman ME, McPherson DD, MacDonald RC. Physical correlates of the ultrasonic reflectivity of lipid dispersions suitable as diagnostic contrast agents. *Ultrasound in Medicine and Biology.* 2002; 28:339–348. [PubMed: 11978414]

47. Negishi Y, Hamano N, Tsunoda Y, Oda Y, Chojjajms B, Endo-Takahashi Y, Omata D, Suzuki R, Maruyama K, Nomizu M, et al. AG73-modified Bubble liposomes for targeted ultrasound imaging of tumor neovasculature. *Biomaterials*. 2013; 34:501–507. [PubMed: 23088840]
48. AlkanOnyuksek H, Demos SM, Lanza GM, Vonesh MJ, Klegerman ME, Kane BJ, Kuszak J, McPherson DD. Development of inherently echogenic liposomes as an ultrasonic contrast agent. *Journal of Pharmaceutical Sciences*. 1996; 85:486–490. [PubMed: 8742939]
49. Wheatley MA, Forsberg F, Oum K, Ro R, El-Sherif D. Comparison of in vitro and in vivo acoustic response of a novel 50:50 PLGA contrast agent. *Ultrasonics*. 2006; 44:360–367. [PubMed: 16730047]
50. Rapoport N, Gao Z, Kennedy A. Multifunctional nanoparticles for combining ultrasonic tumor imaging and targeted chemotherapy. *J Natl Cancer Inst*. 2007; 99:1095–1106. [PubMed: 17623798]
51. Huang SL, Hamilton AJ, Pozharski E, Nagaraj A, Klegerman ME, McPherson DD, MacDonald RC. Physical correlates of the ultrasonic reflectivity of lipid dispersions suitable as diagnostic contrast agents. *Ultrasound Med Biol*. 2002; 28:339–348. [PubMed: 11978414]
52. Huang SL, McPherson DD, Macdonald RC. A method to co-encapsulate gas and drugs in liposomes for ultrasound-controlled drug delivery. *Ultrasound Med Biol*. 2008; 34:1272–1280. [PubMed: 18407399]
53. Mai LY, Yao AN, Li J, Wei Q, Yuchi M, He XL, Ding MY, Zhou QB. Cyanine 5.5 Conjugated Nanobubbles as a Tumor Selective Contrast Agent for Dual Ultrasound-Fluorescence Imaging in a Mouse Model. *Plos One*. 2013; 8
54. Lu Y, Wei J, Shao Q, Tang Y, Huang Y, Zhang H, Yang W, Jing Z. Assessment of atherosclerotic plaques in the rabbit abdominal aorta with interleukin-8 monoclonal antibody-targeted ultrasound microbubbles. *Mol Biol Rep*. 2013; 40:3083–3092. [PubMed: 23292075]
55. Milgroom A, Intrator M, Madhavan K, Mazzaro L, Shandas R, Liu BL, Park D. Mesoporous silica nanoparticles as a breast-cancer targeting ultrasound contrast agent. *Colloids and Surfaces B-Biointerfaces*. 2014; 116:652–657.
56. Klonisch T, Wiechec E, Hombach-Kionisch S, Ande SR, Wesselborg S, Schulze-Osthoff K, Los M. Cancer stem cell markers in common cancers - therapeutic implications. *Trends in Molecular Medicine*. 2008; 14:450–460. [PubMed: 18775674]
57. Kinoshita M, Hynynen K. Intracellular delivery of Bak BH3 peptide by microbubble-enhanced ultrasound. *Pharm Res*. 2005; 22:716–720. [PubMed: 15906165]
58. Miao CH, Brayman AA, Loeb KR, Ye P, Zhou L, Mourad P, Crum LA. Ultrasound enhances gene delivery of human factor IX plasmid. *Hum Gene Ther*. 2005; 16:893–905. [PubMed: 16000070]
59. Bekeredjian R, Katus HA, Kuecherer HF. Therapeutic use of ultrasound targeted microbubble destruction: a review of non-cardiac applications. *Ultraschall Med*. 2006; 27:134–140. [PubMed: 16612722]
60. Kheirrolomoom A, Dayton PA, Lum AF, Little E, Paoli EE, Zheng H, Ferrara KW. Acoustically-active microbubbles conjugated to liposomes: characterization of a proposed drug delivery vehicle. *J Control Release*. 2007; 118:275–284. [PubMed: 17300849]
61. Qiu L, Jing N, Jin Y. Preparation and in vitro evaluation of liposomal chloroquine diphosphate loaded by a transmembrane pH-gradient method. *Int J Pharm*. 2008; 361:56–63. [PubMed: 18573626]
62. Guo X, Szoka FC Jr. Chemical approaches to triggerable lipid vesicles for drug and gene delivery. *Acc Chem Res*. 2003; 36:335–341. [PubMed: 12755643]
63. Meers P. Enzyme-activated targeting of liposomes. *Adv Drug Deliv Rev*. 2001; 53:265–272. [PubMed: 11744171]
64. Kono K, Nakai R, Morimoto K, Takagishi T. Thermosensitive polymer-modified liposomes that release contents around physiological temperature. *Biochim Biophys Acta*. 1999; 1416:239–250. [PubMed: 9889377]
65. Murdan S. Electro-responsive drug delivery from hydrogels. *J Control Release*. 2003; 92:1–17. [PubMed: 14499181]
66. Rapoport N, Pitt WG, Sun H, Nelson JL. Drug delivery in polymeric micelles: from in vitro to in vivo. *J Control Release*. 2003; 91:85–95. [PubMed: 12932640]

67. Schroeder A, Kost J, Barenholz Y. Ultrasound, liposomes, and drug delivery: principles for using ultrasound to control the release of drugs from liposomes. *Chem Phys Lipids*. 2009; 162:1–16. [PubMed: 19703435]
68. Suzuki R, Takizawa T, Negishi Y, Hagsawa K, Tanaka K, Sawamura K, Utoguchi N, Nishioka T, Maruyama K. Gene delivery by combination of novel liposomal bubbles with perfluoropropane and ultrasound. *J Control Release*. 2007; 117:130–136. [PubMed: 17113176]
69. Huang SL, MacDonald RC. Acoustically active liposomes for drug encapsulation and ultrasound-triggered release. *Biochim Biophys Acta*. 2004; 1665:134–141. [PubMed: 15471579]
70. Dromi S, Frenkel V, Luk A, Traugher B, Angstadt M, Bur M, Poff J, Xie J, Libutti SK, Li KC, et al. Pulsed-high intensity focused ultrasound and low temperature-sensitive liposomes for enhanced targeted drug delivery and antitumor effect. *Clin Cancer Res*. 2007; 13:2722–2727. [PubMed: 17473205]
71. Kopechek JA, Abruzzo TM, Wang B, Chrzanowski SM, Smith DA, Kee PH, Huang S, Collier JH, McPherson DD, Holland CK. Ultrasound-mediated release of hydrophilic and lipophilic agents from echogenic liposomes. *J Ultrasound Med*. 2008; 27:1597–1606. [PubMed: 18946099]
72. Rapoport N, Nam KH, Gupta R, Gao Z, Mohan P, Payne A, Todd N, Liu X, Kim T, Shea J, et al. Ultrasound-mediated tumor imaging and nanotherapy using drug loaded, block copolymer stabilized perfluorocarbon nanoemulsions. *J Control Release*. 2011; 153:4–15. [PubMed: 21277919]
73. Gao Z, Kennedy AM, Christensen DA, Rapoport NY. Drug-loaded nano/microbubbles for combining ultrasonography and targeted chemotherapy. *Ultrasonics*. 2008; 48:260–270. [PubMed: 18096196]
74. Fabiilli ML, Haworth KJ, Sebastian IE, Kripfgans OD, Carson PL, Fowlkes JB. Delivery of chlorambucil using an acoustically-triggered perfluoropentane emulsion. *Ultrasound Med Biol*. 2010; 36:1364–1375. [PubMed: 20691925]
75. Fabiilli ML, Lee JA, Kripfgans OD, Carson PL, Fowlkes JB. Delivery of water-soluble drugs using acoustically triggered perfluorocarbon double emulsions. *Pharm Res*. 2010; 27:2753–2765. [PubMed: 20872050]
76. Rapoport N. Phase-shift, stimuli-responsive perfluorocarbon nanodroplets for drug delivery to cancer. *Wiley Interdiscip Rev Nanomed Nanobiotechnol*. 2012; 4:492–510. [PubMed: 22730185]
77. Eisenbrey JR, Soulen MC, Wheatley MA. Delivery of encapsulated Doxorubicin by ultrasound-mediated size reduction of drug-loaded polymer contrast agents. *IEEE Trans Biomed Eng*. 2009; 57:24–28. [PubMed: 19709952]
78. Zhang X, Zheng Y, Wang Z, Huang S, Chen Y, Jiang W, Zhang H, Ding M, Li Q, Xiao X, et al. Methotrexate-loaded PLGA nanobubbles for ultrasound imaging and Synergistic Targeted therapy of residual tumor during HIFU ablation. *Biomaterials*. 2014; 35:5148–5161. [PubMed: 24680663]
79. Eisenbrey JR, Burstein OM, Kambhampati R, Forsberg F, Liu JB, Wheatley MA. Development and optimization of a doxorubicin loaded poly(lactic acid) contrast agent for ultrasound directed drug delivery. *J Control Release*. 2010; 143:38–44. [PubMed: 20060024]
80. Rapoport N, Payne A, Dillon C, Shea J, Scaife C, Gupta R. Focused ultrasound-mediated drug delivery to pancreatic cancer in a mouse model. *Journal of Therapeutic Ultrasound*. 2013; 1
81. Rapoport N, Nam KH, Gupta R, Gao Z, Mohan P, Payne A, Todd N, Liu X, Kim T, Shea J, et al. Ultrasound-mediated tumor imaging and nanotherapy using drug loaded, block copolymer stabilized perfluorocarbon nanoemulsions. *J Control Release*. 153:4–15. [PubMed: 21277919]
82. Cavalli R, Bisazza A, Trotta M, Argenziano M, Civra A, Donalisio M, Lembo D. New chitosan nanobubbles for ultrasound-mediated gene delivery: preparation and in vitro characterization. *Int J Nanomedicine*. 2012; 7:3309–3318. [PubMed: 22802689]
83. Perera RH, Krupka TM, Wu H, Traugher B, Dremann D, Broome AM, Exner AA. Role of Pluronic block copolymers in modulation of heat shock protein 70 expression. *Int J Hyperthermia*. 2011; 27:672–681. [PubMed: 21992560]
84. Weinberg BD, Krupka TM, Haaga JR, Exner AA. Combination of Sensitizing Pretreatment and Radiofrequency Tumor Ablation: Evaluation in Rat Model. *Radiology*. 2008; 246:796–803. [PubMed: 18309015]



85. Javadi M, Pitt WG, Tracy CM, Barrow JR, Willardson BM, Hartley JM, Tsosie NH. Ultrasonic gene and drug delivery using eLiposomes. *J Control Release*. 2013; 167:92–100. [PubMed: 23352908]
86. Lin CY, Javadi M, Belnap DM, Barrow JR, Pitt WG. Ultrasound sensitive eLiposomes containing doxorubicin for drug targeting therapy. *Nanomedicine*. 2013; 10:67–76. [PubMed: 23845926]
87. Yin T, Wang P, Li J, Zheng R, Zheng B, Cheng D, Li R, Lai J, Shuai X. Ultrasound-sensitive siRNA-loaded nanobubbles formed by hetero-assembly of polymeric micelles and liposomes and their therapeutic effect in gliomas. *Biomaterials*. 2013; 34:4532–4543. [PubMed: 23522375]
88. Ke H, Wang J, Dai Z, Jin Y, Qu E, Xing Z, Guo C, Yue X, Liu J. Gold-nanoshelled microcapsules: a theranostic agent for ultrasound contrast imaging and photothermal therapy. *Angew Chem Int Ed Engl*. 2011; 50:3017–3021. [PubMed: 21404389]
89. Ke HT, Wang JR, Tong S, Jin YS, Wang SM, Qu EZ, Bao G, Dai ZF. Gold Nanoshelled Liquid Perfluorocarbon Magnetic Nanocapsules: a Nanotheranostic Platform for Bimodal Ultrasound/Magnetic Resonance Imaging Guided Photothermal Tumor Ablation. *Theranostics*. 2014; 4:12–23. [PubMed: 24396512]
90. Mallidi S, Larson T, Tam J, Joshi PP, Karpouk A, Sokolov K, Emelianov S. Multiwavelength photoacoustic imaging and plasmon resonance coupling of gold nanoparticles for selective detection of cancer. *Nano Lett*. 2009; 9:2825–2831. [PubMed: 19572747]
91. Mallidi S, Larson T, Aaron J, Sokolov K, Emelianov S. Molecular specific optoacoustic imaging with plasmonic nanoparticles. *Opt Express*. 2007; 15:6583–6588. [PubMed: 19546967]
92. Milgroom A, Intrator M, Madhavan K, Mazzaro L, Shandas R, Liu B, Park D. Mesoporous silica nanoparticles as a breast-cancer targeting ultrasound contrast agent. *Colloids Surf B Biointerfaces*. 116:652–657. [PubMed: 24269054]
93. Casciaro S, Conversano F, Ragusa A, Malvindi MA, Franchini R, Greco A, Pellegrino T, Gigli G. Optimal enhancement configuration of silica nanoparticles for ultrasound imaging and automatic detection at conventional diagnostic frequencies. *Invest Radiol*. 2010; 45:715–724. [PubMed: 20562708]
94. Xie M, Shi H, Ma K, Shen H, Li B, Shen S, Wang X, Jin Y. Hybrid nanoparticles for drug delivery and bioimaging: mesoporous silica nanoparticles functionalized with carboxyl groups and a near-infrared fluorescent dye. *J Colloid Interface Sci*. 2013; 395:306–314. [PubMed: 23394807]
95. Chen AM, Zhang M, Wei D, Stueber D, Taratula O, Minko T, He H. Co-delivery of doxorubicin and Bcl-2 siRNA by mesoporous silica nanoparticles enhances the efficacy of chemotherapy in multidrug-resistant cancer cells. *Small*. 2009; 5:2673–2677. [PubMed: 19780069]
96. Lanza GM, Wickline SA. Targeted ultrasonic contrast agents for molecular imaging and therapy. *Curr Probl Cardiol*. 2003; 28:625–653. [PubMed: 14691443]
97. Ke H, Yue X, Wang J, Xing S, Zhang Q, Dai Z, Tian J, Wang S, Jin Y. Gold nanoshelled liquid perfluorocarbon nanocapsules for combined dual modal ultrasound/CT imaging and photothermal therapy of cancer. *Small*. 2014; 10:1220–1227. [PubMed: 24500926]
98. Harvey CJ, Lim AK, Blomley MJ, Taylor-Robinson SD, Gedroyc WM, Cosgrove DO. Detection of an occult hepatocellular carcinoma using ultrasound with liver-specific microbubbles. *Eur Radiol*. 2002; 12(Suppl 3):S70–73. [PubMed: 12522608]
99. Ayida G, Harris P, Kennedy S, Seif M, Barlow D, Chamberlain P. Hysterosalpingo-contrast sonography (HyCoSy) using Echovist-200 in the outpatient investigation of infertility patients. *Br J Radiol*. 1996; 69:910–913. [PubMed: 9038525]
100. Darge K, Riedmiller H. Current status of vesicoureteral reflux diagnosis. *World J Urol*. 2004; 22:88–95. [PubMed: 15173954]
101. Albrecht T, Blomley MJ, Burns PN, Wilson S, Harvey CJ, Leen E, Claudon M, Calliada F, Correias JM, LaFortune M, et al. Improved detection of hepatic metastases with pulse-inversion US during the liver-specific phase of SHU 508A: multicenter study. *Radiology*. 2003; 227:361–370. [PubMed: 12649417]
102. Gandhok NK, Block R, Ostoic T, Rawal M, Hickie P, Devries S, Feinstein SB. Reduced forward output states affect the left ventricular opacification of intravenously administered Albutex. *J Am Soc Echocardiogr*. 1997; 10:25–30. [PubMed: 9046490]

103. Ma, X. Contrast Media and Contrast-Enhanced Ultrasound Evaluation. In: Sahani, D.; Samir, A., editors. *Abdominal Imaging*. 1. Elsevier; 2011.
104. Wilson SR, Greenbaum LD, Goldberg BB. Contrast-enhanced ultrasound: What is the evidence and what are the obstacles? *Am J Roentgen*. 2009; 193:6.
105. Grayburn P. Perflenenapent emulsion (EchoGen): a new long-acting phase-shift agent for contrast echocardiography. *Clin Cardiol*. 1997; 20:112–18. [PubMed: 9383597]
106. Schneider M, Broillet A, Bussat P, Giessinger N, Puginier J, Ventrone R, Yan F. Gray-scale liver enhancement in VX2 tumor-bearing rabbits using BR14, a new ultrasonographic contrast agent. *Investigative Radiology*. 1997; 32:410–417. [PubMed: 9228607]
107. Hirai T. Expectations for contrast-enhanced ultrasonography. *J Med Ultrasonics*. 2014; 41:2.

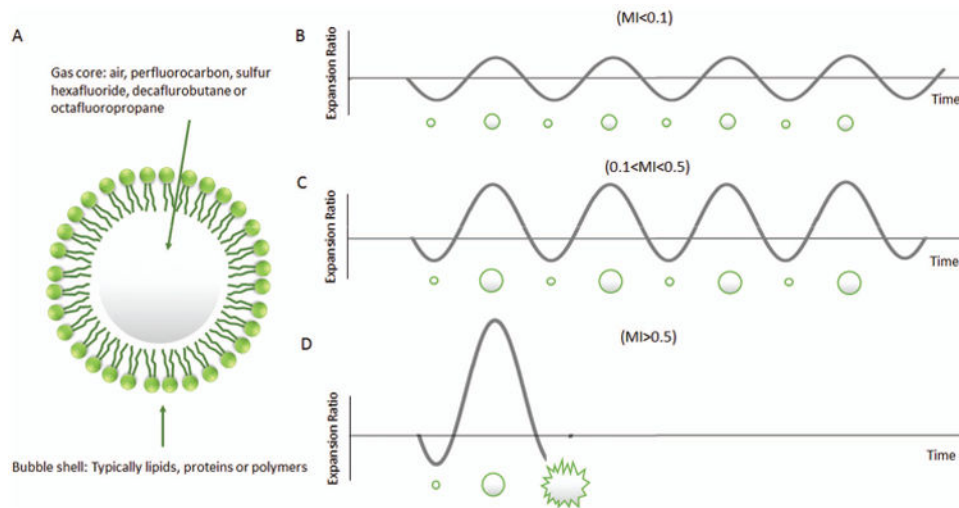


**Figure 1.**

(A) Structure of a microbubble; (B) Microbubble linear oscillation under low acoustic power ( $MI < 0.1$ ); (C) Microbubble nonlinear oscillation under medium acoustic power ( $0.1 < MI < 0.5$ ); (D) Microbubble destruction under high acoustic power ( $MI > 0.5$ ).

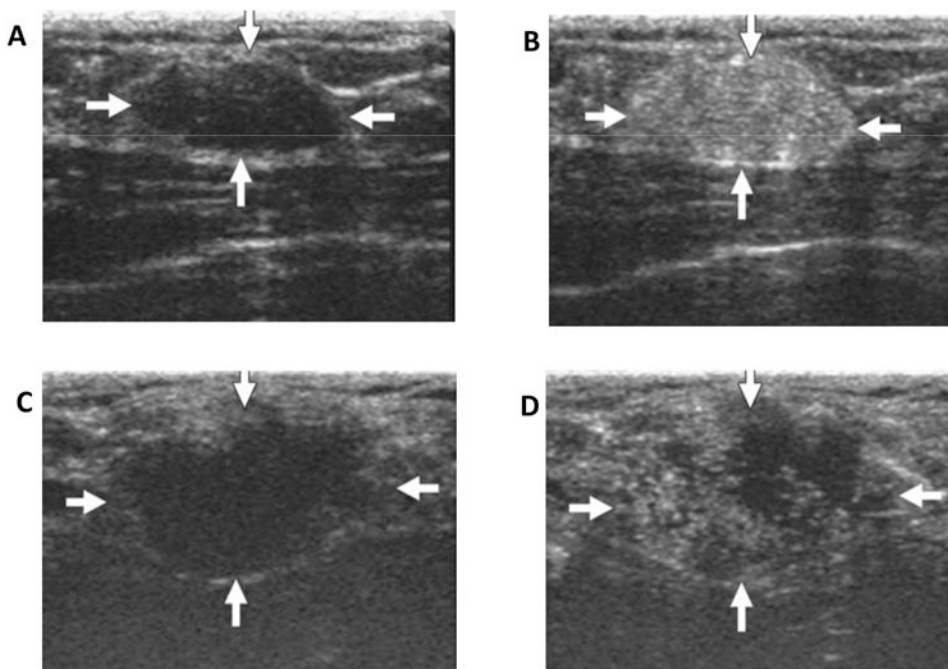


**Figure 2.** (A) Unenhanced ultrasound image shows homogeneously hypoechoic oval shaped solid mass (arrows) in fibroglandular tissue of breast with adenoma (22 years old women); (B) Contrast enhanced ultrasound image of same area; (C) Unenhanced ultrasound image shows lobulated hypoechoic mass (arrows) in fibroglandular tissue of papillotubular carcinoma (38 years old woman); (D) Contrast enhanced ultrasound image of same area shows clear internal defects. (Reprinted from Ref 32. Copyright 2014 Miyamoto, Y. et al – permission pending).

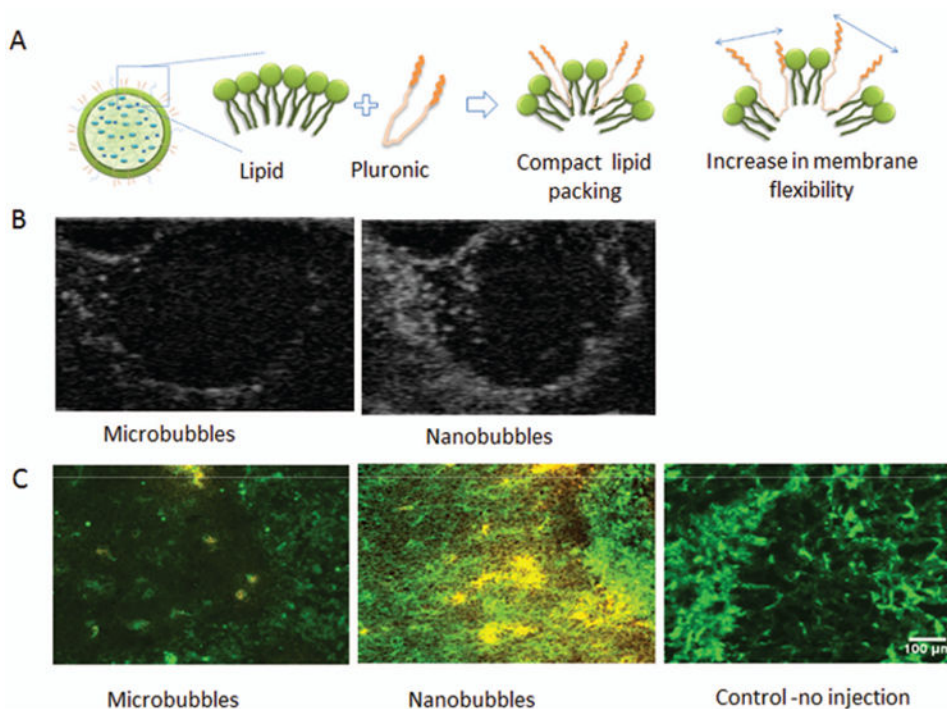


**Figure 3.** (A) Schematic of nanobubbles and functionality of Pluronic in changing lipid packing and increasing membrane flexibility; (B) B-mode images of tumors after nanobubble and control microbubble administration; (C) Histological analysis demonstrating DiI label (yellow color) Pluronic nanobubble extravasation into 4T1 breast cancer tumors compared to DiI labeled microbubbles. CD31 on the vasculature was stained green with FITC antibodies. (Unpublished data).

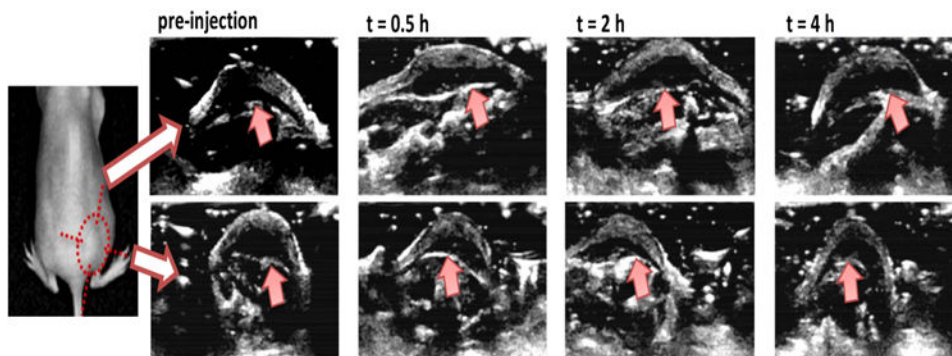


**Figure 4.**

In vivo ultrasound images of subcutaneous tumors with injection of cy5.5-nanobubble suspension. Ultrasound images were obtained with LOGIQ7 system with a thyroid transducer at 12 MHz. Top and bottom panels are images of the same tumor at orthogonal angles. The basal periphery of tumor was indicated with arrows in images (Reprinted from Ref 53. Copyright 2013 Mai et al).

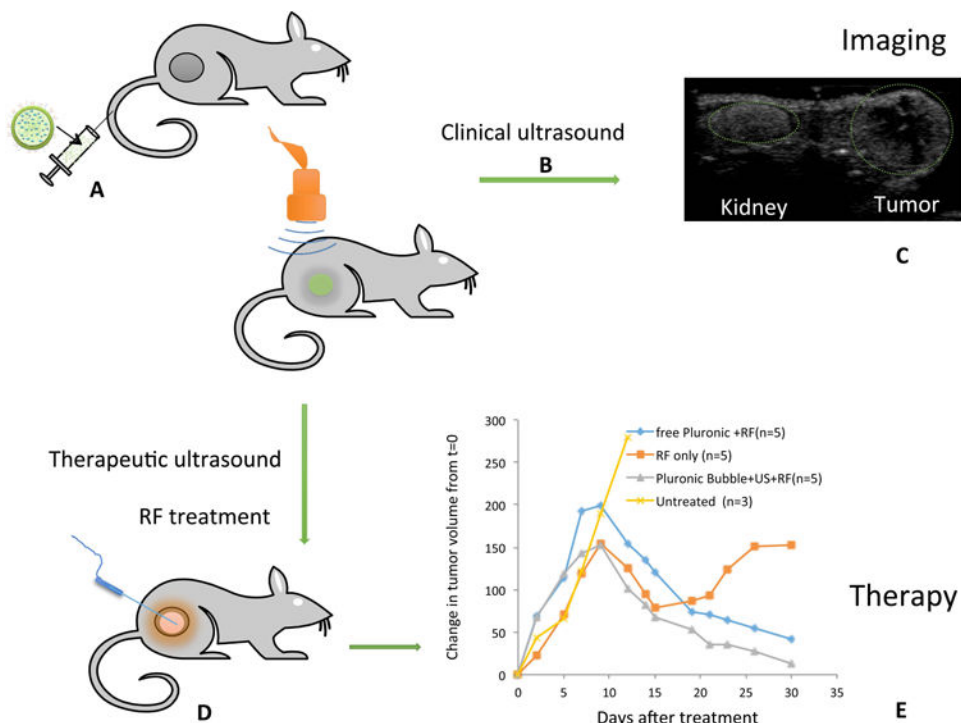


**Figure 5.** Schematic diagram showing the theranostic effect of Pluronic nanobubble (A) Bubble injection; (B) Ultrasound imaging using clinical ultrasound; (C) Representative image showing enhanced contrast of tumor and kidney after bubble injection; (D) Application of therapeutic ultrasound and radiofrequency (RF) ablation; (E) Change in volume of tumors in mice relative to the initial size before the treatment.

Author Manuscript

Author Manuscript

Author Manuscript

Author Manuscript

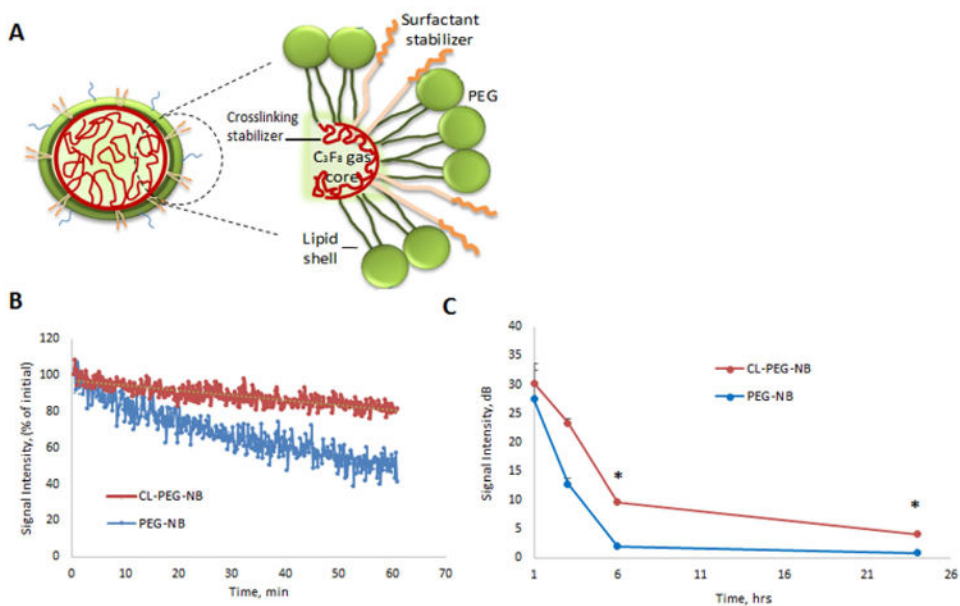


**Figure 6.**

(A) Scheme of the cross-linked stabilized Pluronic nanobubble; (B) Ultrasound decay of crosslinked bubbles (CL-PEG-NB) and non-crosslinked bubbles (PEG-NB) over 1 h; (C) Ultrasound decay rate over 24 h.



**Table 1**  
**Common Ultrasound Contrast Agents**

Agent	Filling Gas	Shell	Clinical Application	Approval
Sonavist (Shering) <sup>98</sup>	Air (Nitrogen)	Cyanoacrylate	Hepatocellular carcinoma	Experimental
Echovist (Shering) <sup>24, 99</sup>		Galactose	Right chambers Tubal and Uterine imaging	EMA <sup>#</sup>
Levovist (Shering) <sup>100, 101</sup>		Galactose	Vesicoureteral reflux Hepatocellular carcinoma	EMA (formerly), Japan; None
Albunex (Molecular Biosystems) <sup>96, 102</sup>		Albumin	Left and right chambers Fallopian tube patency	FDA (formerly)
Myomap (Quadrant) <sup>103</sup>		Albumin	Myocardial perfusion	Experimental
Quantison (Quadrant) <sup>103</sup>		Albumin	Myocardial perfusion	Experimental
Optison (GE Healthcare) <sup>104</sup>		Albumin	Left ventricle Left ventricular endocardial border Carotid plaque neovascularization	FDA, EMA; FDA, EMA; None
Echogen (Sonos Pharmaceuticals) <sup>105</sup>	Perfluorocarbon	Sucrose	Left and right chambers Left ventricular border	EMA (formerly); EMA (formerly)
Definity (Lantheus Medical Imaging) <sup>27, 104</sup>		Phospholipid	Left ventricle; Left ventricular endocardial border	FDA, EMA
Imagent-Imavist (Alliance)		Phospholipid	Left ventricle Left ventricular endocardial border	FDA (formerly)
BR14 (Bracco) <sup>106</sup>		Phospholipid	Tissue perfusion Liver parenchyma	None
Sonazoid (GE Healthcare) <sup>107</sup>		Phospholipid	Focal breast and liver lesions; Prostate cancer	Japan; None
SonoVue (Bracco) <sup>#</sup>		Sulfur hexafluoride	Phospholipid	Left ventricle Doppler of large vessels Small vessels of breast and liver lesions

<sup>#</sup> European Medicines Agency: [http://www.ema.europa.eu/docs/en\\_GB/document\\_library/EPAR\\_-\\_Summary\\_for\\_the\\_public/human/000303/WC500055374.pdf](http://www.ema.europa.eu/docs/en_GB/document_library/EPAR_-_Summary_for_the_public/human/000303/WC500055374.pdf)